

Spinodal Decomposition in Homogeneous and Isotropic Turbulence

Prasad Perlekar,^{1,2} Roberto Benzi,³ Herman J. H. Clercx,¹ David R. Nelson,⁴ and Federico Toschi^{1,5,6}

¹*Department of Physics and J.M. Burgerscentrum, Eindhoven University of Technology, 5600 MB Eindhoven, The Netherlands; and International Collaboration for Turbulence Research*

²*TIFR Centre for Interdisciplinary Sciences, 21 Brundavan Colony, Narsingi, Hyderabad 500075, India*

³*Dipartimento di Fisica and INFN, Università "Tor Vergata", Via della Ricerca Scientifica 1, I-00133 Roma, Italy*

⁴*Lyman Laboratory of Physics, Harvard University, Cambridge, Massachusetts 02138, USA*

⁵*Department of Mathematics and Computer Science, Eindhoven University of Technology, 5600 MB Eindhoven, The Netherlands*

⁶*CNR, Istituto per le Applicazioni del Calcolo, Via dei Taurini 19, 00185 Rome, Italy*

(Received 27 June 2013; published 8 January 2014)

We study the competition between domain coarsening in a symmetric binary mixture below critical temperature and turbulent fluctuations. We find that the coarsening process is arrested in the presence of turbulence. The physics of the process shares remarkable similarities with the behavior of diluted turbulent emulsions and the arrest length scale can be estimated with an argument similar to the one proposed by Kolmogorov and Hinze for the maximal stability diameter of droplets in turbulence. Although, in the absence of flow, the microscopic diffusion constant is negative, turbulence does effectively arrest the inverse cascade of concentration fluctuations by making the low wavelength diffusion constant positive for scales above the Hinze length.

DOI: 10.1103/PhysRevLett.112.014502

PACS numbers: 47.27.-i, 64.75.-g, 81.30.-t

Turbulence is known to strongly increase mixing efficiency. The enhanced mixing properties of turbulence arise due to its multitime and multiscale correlated velocity fluctuations and can be understood in terms of a phenomenological, and scale-dependent, eddy viscosity $\nu_t(\ell) \sim \nu(\ell/\eta)^{4/3}$ (η is the Kolmogorov dissipative scale at which velocity fluctuations are dissipated [1]). At larger inertial length scales, $\ell > \eta$, the effective diffusivity $\nu_t \gg \nu$ where ν is the kinematic viscosity of the quiescent fluid.

A binary liquid mixture cooled below its critical temperature undergoes a phase transition and the mixture separates into phases enriched with its two components. This phenomenon is known as spinodal decomposition [2]. The dynamics of the phase separation can be understood in terms of incompressible Navier-Stokes equations coupled to Cahn-Hilliard or model- B equations describing the binary mixture order parameter (in the absence of turbulence) [3,4]. Using dimensional estimates, the evolution of the phase separation can be divided into three regimes: (a) In the initial state, the coarsening length scale of the phase separating binary mixture grows as $t^{1/3}$ (Lifshitz-Slyozov scaling, [5]). This corresponds to growth dominated by the binary mixture diffusivity and is associated with the evaporation of small droplets at the expense of larger growing ones. (b) At intermediate times, when fluid motion becomes important, viscous dissipation of the fluid balances the pressure ($\nu \nabla^2 \mathbf{u} \sim \nabla p$) which leads to a linear increase $\sim t$ in the coarsening length (viscous scaling, [6]). (c) At final stages, the coarsening length scale grows as $t^{2/3}$ and is governed by the balance of fluid advection with the variations in chemical potential ($\rho \mathbf{u} \cdot \nabla \mathbf{u} \sim \nabla \mu$) (inertial scaling, [7]). This evolution of the coarsening process

has been verified in earlier numerical [8–12] and experimental studies [13].

In this Letter, we study the competition between incompressible turbulence and the coarsening, which leads to a dynamically active statistically steady state [14]. Turbulence twists, folds, and breaks interfaces into smaller domains whereas coarsening leads to domain growth. We show, here, that turbulence leads to an arrest of the coarsening length (see Fig. 1). We present state-of-the-art high-resolution numerical simulations of a symmetric liquid binary mixture in three dimensions in the presence of external turbulent forcing. Our simulations show that the competition between breakup due to turbulence and coagulation due to spinodal decomposition leads to coarsening arrest. We show that the coarsening length scale can be estimated in terms of the Hinze criterion for droplet breakup [15,16] pointing at a common physics behind the processes. Finally, we show that the back reaction of the binary mixture dynamics on the fluid leads to an alteration of the energy cascade.

Early experiments [17,18] used light scattering to investigate the coarsening arrest in high-Schmidt number ($Sc \equiv \nu/D$) mixtures where D is the diffusivity of the binary mixture. These results were later understood by invoking the idea of scale dependent eddy diffusivity [19,20]. There it was argued that the coarsening would proceed inside the viscous-convective range [21] where the fluid viscosity is important, but the diffusivity of the binary mixture can be ignored. More recent numerical simulations in two-dimensions have studied the effect of chaotic or random velocity fields on the Cahn-Hilliard equation and found that the coarsening is indeed arrested [22–24].

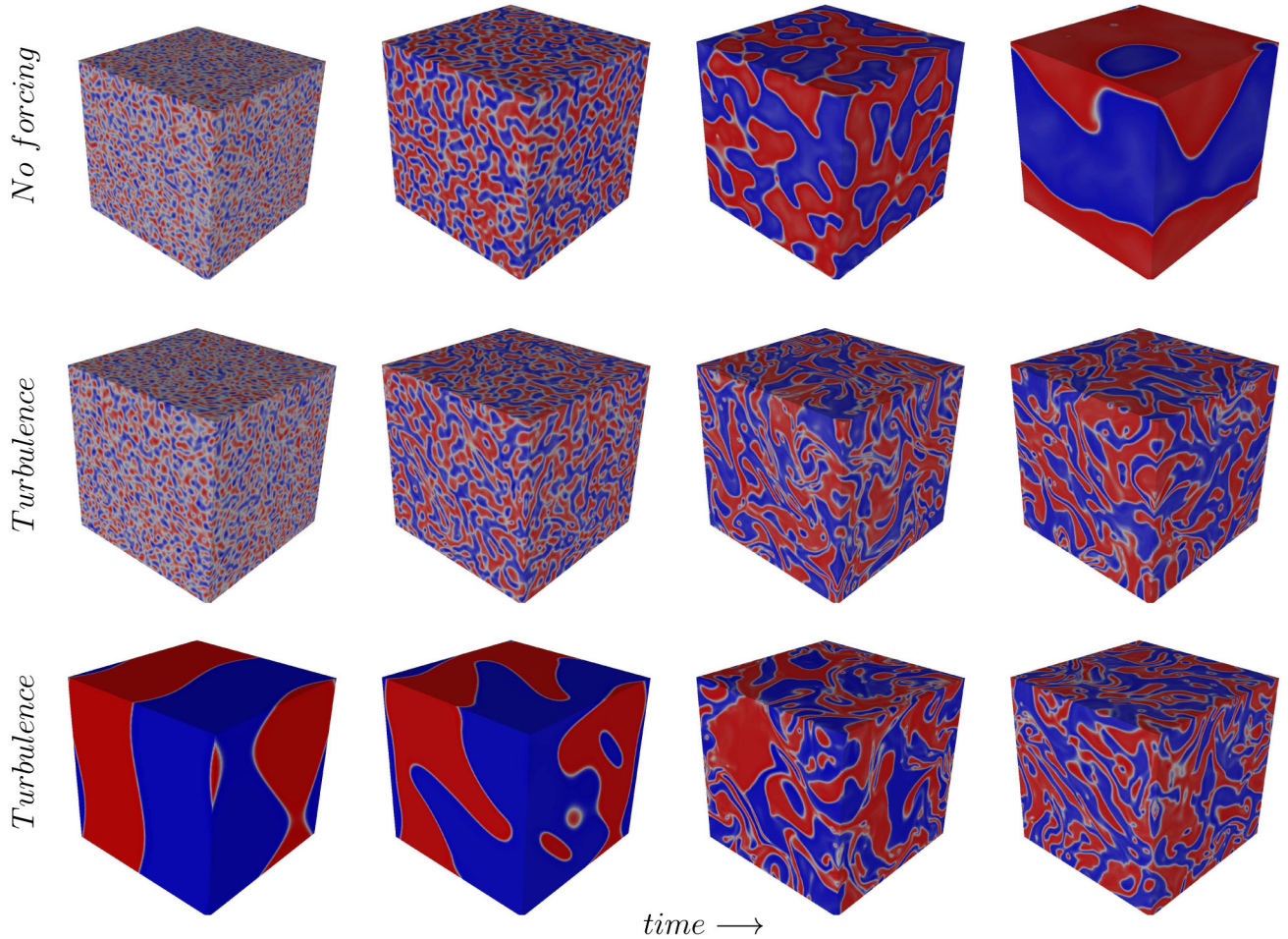


FIG. 1 (color online). Pseudocolor plots of the concentration fields, with the two symmetric fluids indicated in red and blue. (Top panel, left–right) Time evolution of the concentration field undergoing coarsening process from an initially well-mixed state. Notice the formation of ever-larger concentration patches as the time evolves. (Middle panel, left–right) Time evolution of the concentration field undergoing a coarsening process from a well-mixed state in the presence of turbulence generated by external driving. The coarsening process goes on uninhibited until arrested by the turbulence at later times. (Bottom panel, left–right) Time evolution of a very coarse phase-separated mixture in the presence of turbulence with the same intensity as the middle panel. In this case, the domains are broken up until the mixture attains a steady state domain size that is the same as the one in the middle panel. This behavior indicates a positive renormalized eddy diffusivity at large length scales even though the microscopic diffusion constant is negative. The Taylor-microscale Reynolds number for the middle and bottom panels is $Re_\lambda = 103$ (run ST2, Table I). From the plots, it is clear that, in case of turbulence, the coarsening of concentration gets arrested whereas coarsening length attains domain size in the absence of turbulence. In all the panels, the snapshots are taken at times $t = 5.0 \times 10^3$, 1.0×10^4 , 2.5×10^4 , and 1.0×10^5 .

Here, the coarsening length is determined by the balance of the advection of the binary-mixture concentration with gradients in the chemical potential. In Ref. [25], we reported numerical simulations of fully coupled Navier-Stokes and Cahn-Hilliard equations (at $Sc = 0.1$) with externally forced turbulence in two dimensions in the inverse cascade regime. It was shown that the coarsening length varies as $u_{rms}^{-0.41}$, where u_{rms} is the root-mean-square velocity.

In this Letter, we study coarsening arrest in three dimensions using state of the art numerical simulations [16,26]. To simulate binary mixtures we use a two-component Lattice-Boltzmann method [26]. The interaction between the components are introduced using the Shan-Chen

algorithm [26]. Turbulence is generated by using a large-scale sinusoidal forcing along the three directions. All wave modes whose magnitude is less than $\sqrt{2}$ are active and the phases are chosen to be independent Ornstein-Uhlenbeck processes [16].

For all our simulations, we used initial conditions with densities $\rho^{(1)}$ and $\rho^{(2)}$ such that the corresponding initial order parameter field $\phi \equiv (\rho^{(2)} - \rho^{(1)}) / (\rho^{(2)} + \rho^{(1)})$ is a random distribution of $+1$ and -1 . For simulations with turbulence, the forcing was also switched on at the initial time. We simulate in a cubic domain with periodic boundary conditions on all sides. Table I lists the parameters used in our simulations.

TABLE I. The parameters of our simulations. Runs S1–S3 explore spinodal decomposition in the absence of an external forcing, while ST1–ST4 simulate spinodal decomposition in the presence of external driving that generates turbulence. For comparing a turbulent binary mixture with the standard, single-component turbulent fluid (i.e., symmetric binary mixture above its critical point, without surface tension), we also conducted runs NS1 and NS2. The total density of the binary mixture is $\rho = \rho^{(1)} + \rho^{(2)}$. For all the runs, the kinematic viscosity $\nu = 5 \times 10^{-3}$. For runs S1–S3, ST1–3, surface tension $\sigma = 1.6 \times 10^{-3}$, and the Schmidt number $Sc = 1.47$ whereas, for the run ST4, $\sigma = 1.7 \times 10^{-3}$, and $Sc = 3.72$. The Taylor scale Reynolds number is $Re_\lambda \equiv \sqrt{10E}/(\sqrt{\epsilon\nu})$. Here E is the kinetic energy of the fluid and ϵ is the energy dissipation rate.

Runs	Domain size	ρ	Re_λ
S1	128^3	2.4	NA
S2	256^3	2.4	NA
S3	256^3	1.1	NA
ST1	128^3	2.4	35,49
ST2	256^3	2.4	72,103
ST3	512^3	2.4	103,162,185
ST4	256^3	1.1	86
NS1	256^3	2.4	103
NS2	512^3	2.4	162

We first investigate how the coarsening proceeds in absence of turbulence in the viscous scaling regime (runs S1–S3). As a definition of the coarsening length scale $L(t)$, we use $L(t) = 2\pi/[k_1(t)]$, with $k_1(t) = (\sum_k k S_k)/(\sum_k S_k)$, and $S_k = (\sum_k |\phi_k|^2)/(\sum_k 1)$. Here ϕ_k is the Fourier transform of φ , S_k is the shell-averaged concentration spectrum normalized by the corresponding density of states. For the sake of brevity we will call S_k the concentration spectrum. Finally, $k = \sqrt{\mathbf{k} \cdot \mathbf{k}}$, and \sum' indicates the summation over all the modes $k \in [k - 1/2, k + 1/2]$. Below the critical point, phase separation leads to an $L(t)$ that grows with time.

For our runs S1–S3, as expected [6], we observe $L(t) \sim t$ [Fig. 2, (red dots)].

We now study the effect of turbulence on coarsening. We force large length scales to generate homogeneous, isotropic turbulence in the velocity field. In what follows, we study the effect of turbulence in the viscous scaling regime. Note that $Sc = \nu/|D| \sim \mathcal{O}(1)$ in our simulations, whereas for most liquid binary mixtures $Sc \gg 1$, which requires the resolution of both the inertial and the viscous-convective scales to be much higher than what is attained in the present investigation.

Figure 2 shows how $L(t)$ increases in the presence of turbulence. Instead of coarsening until $L(t)$ reaches the size of the simulation domain, turbulence arrests the inverse cascade of concentration fluctuations, blocks coarsening, and leads to a steady state length where the domains constantly undergo coalescence and breakup. The saturating

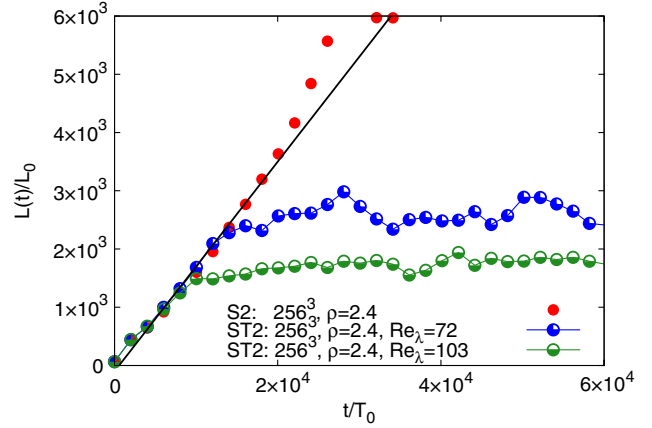


FIG. 2 (color online). Coarsening arrest for phase separating binary mixtures in the presence of turbulence. In the absence of an external turbulent forcing (red circles), the coarsening length keeps on growing as $L(t) \sim t$ (black line). Switching on turbulence, the coarsening length initially grows undisturbed, but then, it arrests as the system attains a steady state. The time and length scale are nondimensionalized by the corresponding characteristic length $L_0 = \nu^2/(\rho\sigma)$ and time $T_0 = \nu^3/(\rho\sigma^2)$.

coarsening length L_∞ decreases with increasing turbulence intensity.

In an earlier study [16], we had shown that, for asymmetric binary mixtures, the Hinze criterion provides an estimate for the average droplet diameter undergoing breakup and coalescence in turbulence. We now show that even for

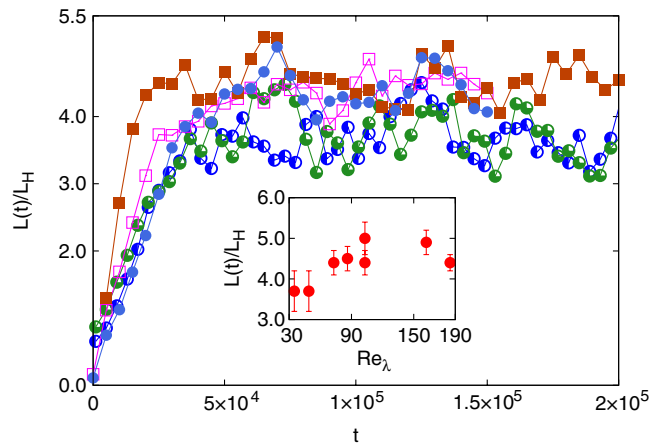


FIG. 3 (color online). Growth of the coarsening length scale $L(t)$ in the arrested state normalized by the Hinze length L_H for $Re_\lambda = 35, 49$ (blue three-quarter-filled circle and green half-filled circle) [run ST1], $Re_\lambda = 72, 103$ (purple square and brown filled square) [run ST2], and $Re_\lambda = 86$ (blue filled circle) [run ST4]. In the inset, we plot the average value of $L(t)/L_H$, calculated over the time window $t = 5 \times 10^4$ to 2×10^5 , for different Reynolds numbers Re_λ . Within error bars, $L(t)/L_H \approx 4.4 \pm 0.5$ is found to be a good indicator for the arrested length scale. We believe that the smaller value of $L(t)/L_H$ (although within our error bars) for the $Re_\lambda = 35, 49$ arises because of the lower grid resolution.

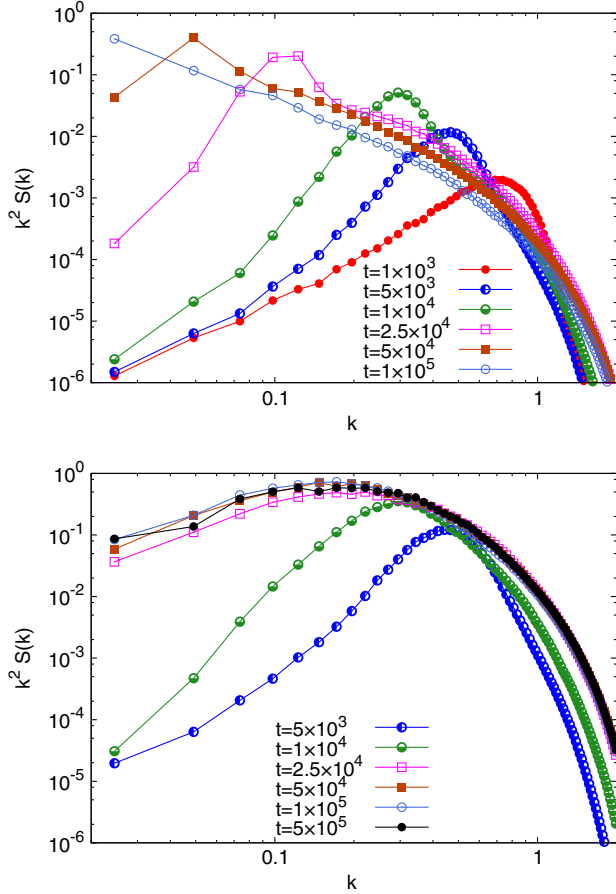


FIG. 4 (color online). (Top panel) The inverse cascade of concentration spectrum $k^2 S(k)$ for spinodal decomposition at times $t = 10^3 - 5 \times 10^5$ (256^3 , $\rho = 2.4$ [run S2]) without turbulence. The Fourier mode associated with the peak of the spectrum gives an estimate of the instantaneous coarsening length. On the other hand, in the presence of turbulence (bottom panel, $\{256^3, \rho = 2.4, \text{ and } \text{Re}_\lambda = 103\}$ [run ST2]), we do observe an initial inverse cascade of concentration that saturates around $t = 5 \times 10^4$ indicating a blockage of the inverse cascade.

50%–50% binary mixtures, the Hinze criterion gives a good estimate for the coarsening length scale L_∞ at long times.

According to the prediction of Ref. [15], the maximum droplet diameter that can be stable to turbulent velocity fluctuations in the steady state should be given by the Hinze length

$$L_H \approx \left(\frac{\rho}{\sigma}\right)^{-3/5} \epsilon^{-2/5}. \quad (1)$$

Actually, the above equation is also consistent with the predictions of Ref. [27]. A general criteria for the coarsening length is given by the relation $L(t) = L_0 f(x)$ with $x = t/T_0$ [27]. The function $f(x)$ satisfies the two limiting scaling $f(x) \sim x$ for small x and $f(x) \sim x^{2/3}$ for large x . In turbulent flow, the relevant time scale is given by $L/\delta v(L)$

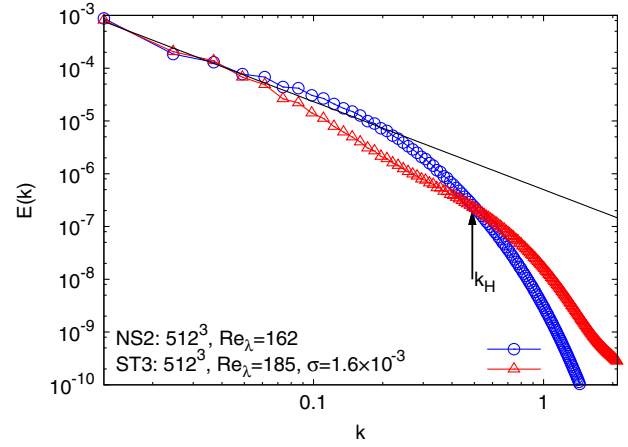


FIG. 5 (color online). Comparison of the energy spectrum for the spinodal decomposition in the presence of turbulence (triangle, run ST3 [$\text{Re}_\lambda = 185$]) with the pure fluid case (circle, run NS2). The black line indicates the Kolmogorov scaling $k^{-5/3}$. We find that the large- k crossover takes place roughly around the inverse Hinze scale $k_H \equiv 1/L_H$. This crossover was also confirmed by comparing runs NS1 and ST2 (not shown here).

where $\delta v(L)$ is the size of the velocity fluctuation at the scale L . Since this time scale is much longer than t , the appropriate scaling behavior for $f(x)$ is $x^{2/3}$. Using the inertial scaling, we again obtain Eq. (1). The above argument may not apply to shear flows, due to nonisotropic contributions and strong dissipation at the boundaries, and in two dimensional flows where the characteristic time scale is dictated by enstrophy cascade.

In [16,28], it was shown that in the presence of coagulation-breakup processes the correct quantity to look at is the average droplet diameter $L_\infty \equiv \langle L(t) \rangle$ in the statistically stationary state. Therefore, we expect that the ratio $L(t)/L_H$ stays constant in all our simulations. The plot in Fig. 3 shows the plot of $L(t)/L_H$ for our runs.

The blockage of the energy transfer by turbulence is best understood in Fourier space. The plots in Fig. 4 compare the concentration spectrum $k^2 S_k$ at various times $t = 10^3, 10^4$, and 10^5 in the absence ($256^3, \rho = 2.4$ [run S2]) and presence ($256^3, \rho = 2.4$, and $\text{Re}_\lambda = 103$ [run ST2]) of turbulence. Without turbulence, we observe a peak in the concentration spectrum at initial times that moves towards smaller wave vectors until it reaches the domain size. On the other hand, in the presence of turbulence, the concentration fluctuations saturate, and the concentration spectrum reaches a steady state.

The presence of a surface tension should also alter the transfer of energy in Fourier space. On the other hand, in the regions of weak turbulence, local chemical potential will transfer energy back to the fluid. In Fig. 5, we investigate how a phase separating binary liquid mixture velocity spectrum compares with the pure fluid case. We observe that in the inertial range the energy content of the binary

mixture is strongly suppressed in comparison to the pure fluid case, whereas in the dissipation range, the energy content is higher for the binary mixture.

We acknowledge the COST Action MP0806 and FOM (Stichting voor Fundamenteel Onderzoek der Materie) for support. We acknowledge computational support from CASPUR (Roma, Italy), from CINECA (Bologna, Italy), and from JSC (Juelich, Germany). This research was supported in part by the National Science Foundation under Grant No. PHY11-25915. Work by D. R. N. was supported by the National Science Foundation (USA) via Grant No. DMR 1005289 and through the Harvard Materials Research Science and Engineering Laboratory, through Grant No. DMR 0820484.

-
- [1] W. Richardson, *Proc. R. Soc. A* **110**, 709 (1926).
 [2] K. Dill and S. Bromberg, *Molecular Driving Forces* (Garland Science, New York, 2003).
 [3] J. Cahn, *Trans. Metall. Soc. AIME* **242**, 166 (1968).
 [4] P. Hohenburg and B. Halperin, *Rev. Mod. Phys.* **49**, 435 (1977).
 [5] I. Lifshitz and V. Slyozov, *J. Phys. Chem. Solids* **19**, 35 (1961).
 [6] E. D. Siggia, *Phys. Rev. A* **20**, 595 (1979).
 [7] H. Furukawa, *Phys. Rev. A* **31**, 1103 (1985).
 [8] T. Lookman, Y. Wu, F. J. Alexander, and S. Chen, *Phys. Rev. E* **53**, 5513 (1996).
 [9] V. M. Kendon, *Phys. Rev. E* **61**, R6071 (2000).
 [10] I. Pagonabarraga, J.-C. Desplat, A. J. Wagner, and M. E. Cates, *New J. Phys.* **3**, 9 (2001).
 [11] N. Gonzalez-Segredo, M. Nekovee, and P. V. Coveney, *Phys. Rev. E* **67**, 046304 (2003).
 [12] G. Gonnella and J. M. Yeomans, in *Kinetics of Phase Transitions*, edited by S. Puri and V. Wadhawan (CRC Press, Boca Raton, 2009), p. 121.
 [13] J. Hogley, S. Kajimoto, A. Takamizawa, and H. Fukumura, *Phys. Rev. E* **73**, 011502 (2006).
 [14] R. Ruiz and D. R. Nelson, *Phys. Rev. A* **23**, 3224 (1981).
 [15] J. Hinze, *AIChE J.* **1**, 289 (1955).
 [16] P. Perlekar, L. Biferale, M. Sbragaglia, S. Srivastava, and F. Toschi, *Phys. Fluids* **24**, 065101 (2012).
 [17] D. J. Pine, N. Easwar, J. V. Maher, and W. I. Goldberg, *Phys. Rev. A* **29**, 308 (1984).
 [18] P. Tong, W. I. Goldberg, J. Stavans, and A. Onuki, *Phys. Rev. Lett.* **62**, 2668 (1989).
 [19] Ref. 20 uses the Prandtl number instead of the Schmidt number. To be consistent with the mixing of a scalar in turbulence we use the Schmidt number.
 [20] J. A. Aronovitz and D. R. Nelson, *Phys. Rev. A* **29**, 2012 (1984).
 [21] G. Batchelor, *J. Fluid Mech.* **5**, 113 (1959).
 [22] A. M. Lacasta, J. M. Sancho, and F. Sagues, *Phys. Rev. Lett.* **75**, 1791 (1995).
 [23] L. Berthier, J. L. Barrat, and J. Kurchan, *Phys. Rev. Lett.* **86**, 2014 (2001).
 [24] L. ÓNáirigh and J. L. Thiffeault, *Phys. Rev. E* **75**, 016216 (2007).
 [25] S. Berti, G. Boffetta, M. Cencini, and A. Vulpiani, *Phys. Rev. Lett.* **95**, 224501 (2005).
 [26] X. Shan and H. Chen, *Phys. Rev. E* **47**, 1815 (1993); *Phys. Rev. E* **49**, 2941 (1994).
 [27] M. Cates, arXiv:1209.2290.
 [28] L. Biferale, P. Perlekar, M. Sbragaglia, S. Srivastava, and F. Toschi, *J. Phys. Conf. Ser.* **318**, 052017 (2011).